

Rewiring the taste system

Hojoon Lee^{1,2*}, Lindsey J. Macpherson^{1,2*}, Camilo A. Parada^{1,2}, Charles S. Zuker^{1,2} & Nicholas J. P. Ryba³

In mammals, taste buds typically contain 50–100 tightly packed taste-receptor cells (TRCs), representing all five basic qualities: sweet, sour, bitter, salty and umami^{1,2}. Notably, mature taste cells have life spans of only 5–20 days and, consequently, are constantly replenished by differentiation of taste stem cells³. Given the importance of establishing and maintaining appropriate connectivity between TRCs and their partner ganglion neurons (that is, ensuring that a labelled line from sweet TRCs connects to sweet neurons, bitter TRCs to bitter neurons, sour to sour, and so on), we examined how new connections are specified to retain fidelity of signal transmission. Here we show that bitter and sweet TRCs provide instructive signals to bitter and sweet target neurons via different guidance molecules (SEMA3A and SEMA7A)^{4–6}. We demonstrate that targeted expression of SEMA3A or SEMA7A in different classes of TRCs produces peripheral taste systems with miswired sweet or bitter cells. Indeed, we engineered mice with bitter neurons that now responded to sweet tastants, sweet neurons that responded to bitter or sweet neurons responding to sour stimuli. Together, these results uncover the basic logic of the wiring of the taste system at the periphery, and illustrate how a labelled-line sensory circuit preserves signalling integrity despite rapid and stochastic turnover of receptor cells.

Unlike the wiring of the mammalian olfactory system, where odorant receptors have a key role in directing connectivity between olfactory neurons and their targets in the olfactory bulb^{7,8}, taste receptors themselves are not essential for establishing connectivity between TRCs and their targets (that is, TRCs lacking taste receptors still signal properly when expressing engineered receptors^{9,10}). Thus, we reasoned that as new TRCs are produced, they must express dedicated molecular cues that act as permissive and/or instructive signals⁴ to establish connectivity with the right complement of taste neurons (Fig. 1a).

We isolated sweet and bitter TRCs (see Methods for details), performed RNA-sequencing (RNA-seq) and searched for candidate proteins that could potentially serve to specify the wiring of labelled lines (for example, adhesion molecules, growth factors, axon guidance molecules or synaptic components)^{11–13}. In this analysis, bitter cells were readily identified by the high levels of expression of bitter taste receptors¹⁰ (Fig. 1b, green symbols), while sweet TRCs were characterized by the presence of subunits of the sweet receptor⁹ (Fig. 1b, blue symbols). Several candidate molecules were differentially expressed between classes of TRCs, including semaphorins, protocadherin and DSCAMs^{11–13} (Fig. 1b, Extended Data Fig. 1d and Supplementary Table 1).

Semaphorin 3A (SEMA3A), a known connectivity molecule^{5,6}, was enriched more than 100-fold in bitter TRCs versus other cells types (Fig. 1b, c). Semaphorins are a large family of membrane-associated and secreted proteins that are widely expressed throughout the nervous system, and are often implicated in axon guidance, neural circuit assembly and synaptic refinement^{13–15}. SEMA3A, in particular, was first identified as a secreted repulsive axon guidance signal mediating

growth cone collapse^{16,17}, but more recently it has also been implicated in chemoattraction^{18–20}.

To probe the specificity of the ‘handshake’ between bitter ganglion neurons and TRCs, we performed *in vivo* functional calcium imaging experiments (see ref. 21). In essence, since the taste selectivity of ganglion neurons reflects the identity of the TRCs they connect to (for example, sweet TRCs, bitter TRCs, and so on), by recording the responses of ganglion neurons to stimulation of the tongue with all 5 tastes, we can directly infer their corresponding TRC input^{21,22}. Therefore, we targeted the calcium indicator GCaMP6s to geniculate ganglion neurons using retrograde viral transduction, exposed a small imaging window through the tympanic bulla to allow optical access to the entire ganglion *in vivo*, and assessed the tuning properties of taste neurons using bitter, sweet, sour, salt and umami stimuli (see Methods for details). In wild-type controls, the vast majority of geniculate ganglion neurons respond to a single taste quality²¹ (Fig. 2a–c). For example, over 90% of bitter-responsive neurons receive input from only bitter TRCs (see Fig. 2c).

How do bitter ganglion neurons, which do not turn over, recognize and reconnect to bitter taste receptor cells that are continuously turning over? To investigate the role of SEMA3A in bitter TRCs, we engineered mice with a conditional deletion of *Sema3a* in bitter TRCs (*Sema3a*^{flx/flx} crossed with *T2r19-cre* (also known as *Tas2r119-cre*)^{10,23}. Figure 2 shows that loss of SEMA3A markedly changed the responses of bitter neurons, such that nearly half of all bitter-responsive neurons were now also activated by other tastants, including sweet, umami and salt (Fig. 2d–f). These results suggest at least two possibilities. Firstly, SEMA3A, which is normally secreted by bitter TRCs, acts as an attractive signal to guide connectivity between bitter TRCs and bitter ganglion neurons. Alternatively, SEMA3A acts as a repulsive signal, preventing incorrect connections between bitter TRCs and non-bitter ganglion neurons.

We reasoned that if SEMA3A functions as an attractive local signal released from bitter TRCs, we may be able to rewire and redirect bitter neurons to another class of TRC by misexpressing SEMA3A ectopically in those cells (Fig. 3a). Therefore, we engineered a mouse line that expresses human SEMA3A in sweet (and umami) cells using the upstream regulatory regions of the sweet/umami T1R3 receptor subunit (*T1r3::SEMA3A* (also known as *Tas1r3::SEMA3A*), see Extended Data Fig. 3a). We hypothesized that bitter ganglion neurons would now be ‘attracted’ to sweet TRCs and that there consequently should be a selective emergence of bitter–sweet ganglion neurons. Indeed, there is a sevenfold increase in the population of bitter–sweet doubly tuned cells (from background levels in controls to over 20% in *T1r3::SEMA3A*, Fig. 3b, c). Moreover, unlike *Sema3a*-knockout mice that have multi-tuned cells across all taste qualities (for example, bitter–salty, bitter–sweet–salty), the bitter phenotype of the misexpressed animals is largely restricted to bitter–sweet.

The misexpression studies described above used engineered mice that still carry wild-type copies of SEMA3A. We anticipated that

¹Howard Hughes Medical Institute, Department of Biochemistry and Molecular Biophysics, Columbia College of Physicians and Surgeons, Columbia University, New York, New York 10032, USA.

²Howard Hughes Medical Institute, Department of Neuroscience, Columbia College of Physicians and Surgeons, Columbia University, New York, New York 10032, USA. ³National Institute of Dental and Craniofacial Research, National Institutes of Health, Bethesda, Maryland 20892, USA.

*These authors contributed equally to this work.

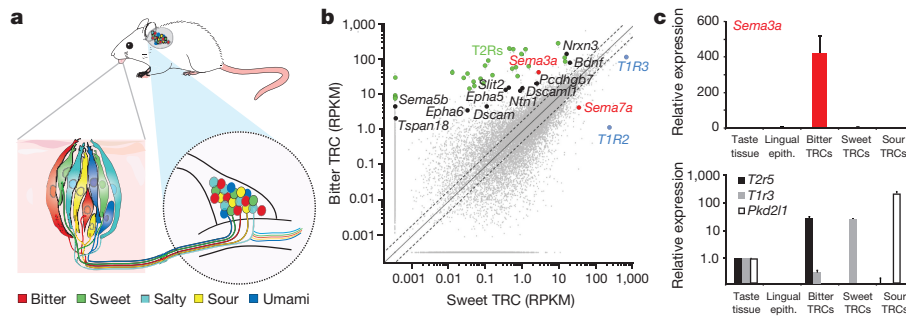


Figure 1 | SEMA3A is expressed in bitter TRCs. **a**, Anatomy of the taste system at the periphery. The lower insets illustrate the labelled lines connecting the different TRCs in a fungiform papillae to matching geniculate ganglion neurons. **b**, RNA-seq data plotting the normalized number of reads (RPKM) in bitter TRCs (TRPM5-BFP⁺;T2R-GFP⁺ double-labelled cells) versus in sweet/umami TRCs (TRPM5-BFP⁺; T2R-GFP⁻); see Extended Data Fig. 1. Coloured dots indicate transcripts of interest, including members of the T2R family of bitter taste receptors (green); *T1r2* (also known as *Tas1r2*) and *T1r3* (also known as *Tas1r3*) (blue), and candidate connectivity molecules enriched in bitter TRCs

(black). SEMA3A and SEMA7A are labelled in red. **c**, Quantitative RT-PCR shows highly selective expression of *Sema3a* in bitter TRCs. Lower panel validates the identity of each TRC population that was obtained with fluorescence-activated cell sorting (FACS) with dedicated TRC marker genes. *T2r5* is also known as *Tas2r105*. Data are presented as mean + s.e.m. relative to the expression levels in the taste tissue (circumvallate papilla); *n* = 3. Expression data for candidate semaphorin receptors in geniculate ganglion neurons are shown in Extended Data Fig. 2.

completely removing functional SEMA3A (ref. 24) from bitter cells should further decrease the remaining number of ‘properly wired’ (singly tuned) bitter cells in the sweet-expressing SEMA3A mice (*T1r3::SEMA3A;Sema3a^{M/M}*, Fig. 3d). As predicted, misexpression in the mutant background leads to a marked reduction of the remaining singly tuned bitter cells (Fig. 3e, from around 50% in the misexpressed mice to 30% in the misexpressed mice that also lack functional endogenous SEMA3A). Of note, even in the absence of functional SEMA3A in bitter TRCs, ganglion neurons can still connect to bitter cells, indicating that additional cues must guide their targeting to bitter TRCs.

Given that in *T1r3::SEMA3A;Sema3a^{M/M}* animals, 70% of bitter-responding neurons are multi-tuned (Fig. 3e), we examined the behavioural responses of these mice to bitter stimuli. Indeed, our results showed that sensitivity to bitter chemicals was markedly impaired, with mutant mice exhibiting compromised aversive responses (Fig. 3f and Extended Data Fig. 5).

The results described above validate SEMA3A as a key mediator of connectivity between bitter TRCs and their partner ganglion neurons. What about the wiring between sweet-TRCs and sweet ganglion neurons? Are similar rules guiding their handshake during the constant

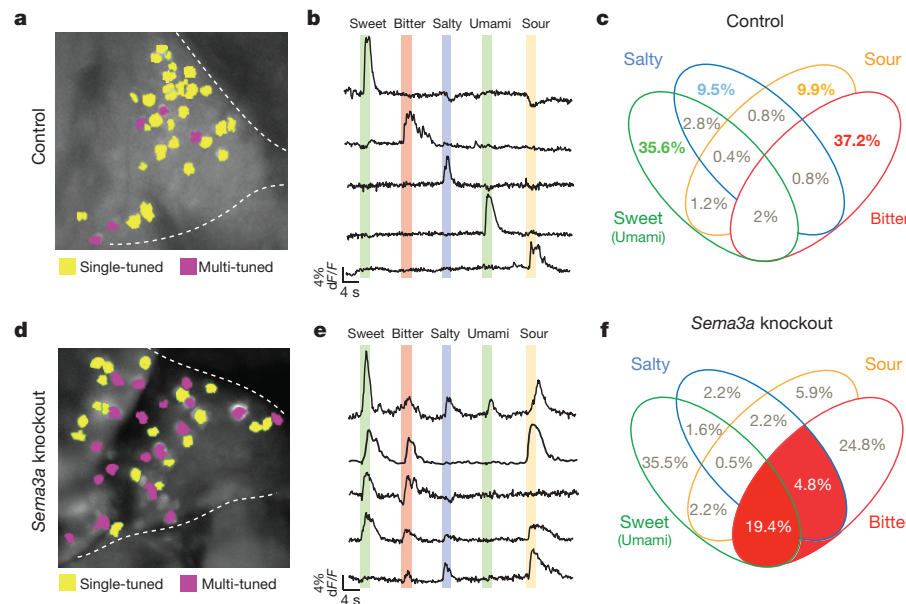


Figure 2 | Removal of SEMA3A from bitter TRCs increases the population of multi-tuned bitter geniculate neurons. **a**, Image of a representative control geniculate ganglion expressing GCaMP6s, highlighting neurons that respond to a single taste quality (yellow) and the small number of neurons that are multi-tuned (magenta). Dashed lines outline the geniculate ganglion with the facial nerve to bottom. **b**, Traces from five separate neurons (from **a**) illustrating the time course and amplitude changes in GCaMP6s signals (*dF/F*) during taste stimulation: sweet (acesulfame K, 30 mM), bitter (quinine, 5 mM), salty (NaCl, 60 mM), umami (monopotassium glutamate 50 mM and inosine monophosphate 1 mM) and sour (citric acid, 50 mM). Coloured bars mark the time and duration (2 s) of the stimulus. Note the specificity of the responses to single taste qualities. **c**, Venn diagram displaying all

possible combinations of tuning properties in control mice, with numbers of neurons in each class indicated as the percentage of the total. Note that over 90% of all neurons are singly tuned. Because there are very few umami-responding neurons in the mouse geniculate ganglion (see ref. 21), we grouped sweet and umami cells in our analysis. Bitter-sour segments are merged as nearly all neurons responding to bitter and sour stimuli represent bitter TRCs that are sensitive to acid²¹; *n* = 13 mice, 254 cells. **d-f**, As in **a-c** for mice in which *Sema3a* was conditionally knocked out in bitter TRCs (*T2r19-cre;Sema3a^{flx/flx}*). Note the marked increase in bitter multi-tuned neurons (highlighted in red in **f**; *n* = 5 mice, 186 cells. See also Extended Data Table 1. Fisher’s exact test: *P* < 0.01 (19.4% versus 2%) and *P* < 0.05 (4.8% versus 0.8%).

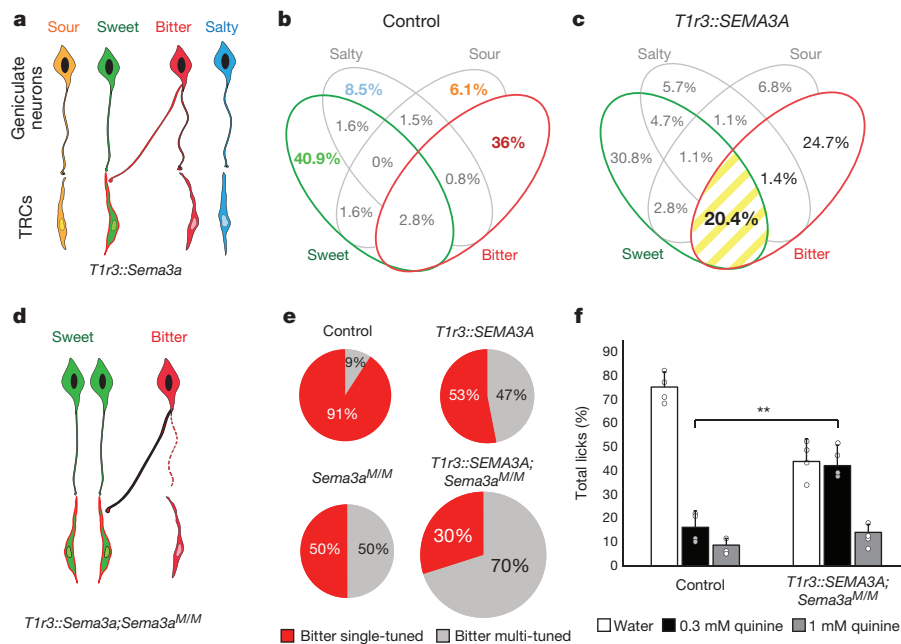


Figure 3 | Rewiring of bitter geniculate ganglion neurons. **a**, Directed misexpression of *SEMA3A* in sweet TRCs targets bitter neurons to sweet TRCs. **b**, **c**, Venn diagram displaying ganglion neuron tuning in control ($n = 9$ mice, 247 cells) and *T1r3::SEMA3A* animals ($n = 6$ mice, 270 cells); numbers of neurons in each class are indicated as the percentage of the total. The large increase in bitter–sweet multi-tuned cells is highlighted in yellow ($P < 0.01$, Fisher’s exact test). **d**, Directed misexpression of *SEMA3A* in sweet TRCs of *SEMA3A*-mutant mice. **e**, Pie charts depicting the fraction of singly (red) and multi-tuned (grey) bitter-responsive neurons in the four different genetic backgrounds. Note the pronounced loss of singly tuned bitter cells in the *T1r3::SEMA3A;Sema3a^{M/M}* double

mutant (*T1r3::SEMA3A;Sema3a^{M/M}* versus others: $P < 0.01$, Fisher’s exact test). Data for control and *T1r3::SEMA3A* are from **b** and **c**, respectively. *Sema3a^{M/M}*, $n = 9$ mice (263 cells); *T1r3::SEMA3A;Sema3a^{M/M}*, $n = 9$ mice (130 cells); see also Extended Data Table 2 and Extended Data Fig. 4. **f**, Animals with bitter neurons rewired to sweet TRCs exhibit a significant loss of bitter taste sensitivity. Mice were presented with water, 0.3 mM quinine and 1 mM quinine; shown are the relative fraction of licks to each stimulus in mutant mice and wild-type controls ($n = 4$; mean \pm s.d.; $**P < 0.01$, Student’s two-tailed, unpaired *t*-test). Unlike controls, the mutant animals failed to distinguish moderate concentrations of bitter from water; see Extended Data Fig. 5 for additional bitters.

renewal of sweet TRCs? We searched for candidate molecules that may mediate the connectivity between sweet TRCs and sweet ganglion neurons. Our expression profiling studies (Figs 1b, 4a–b) singled-out *SEMA7A*, a membrane-bound member of the semaphorin family^{25,26}, as highly selective for sweet cells. To investigate the role of *SEMA7A* in guiding sweet TRC–ganglion connectivity, we engineered mice that

misexpress human *SEMA7A* in bitter TRCs (Extended Data Fig. 3). We reasoned that if *SEMA7A* acts in sweet cells as an instructive signal to sweet ganglion neurons (like *SEMA3A* from bitter TRCs does to bitter ganglion neurons), then the peripheral taste system of animals misexpressing *SEMA7A* in bitter TRCs should now result in a re-routing of sweet ganglion connections to bitter TRCs. As predicted, our

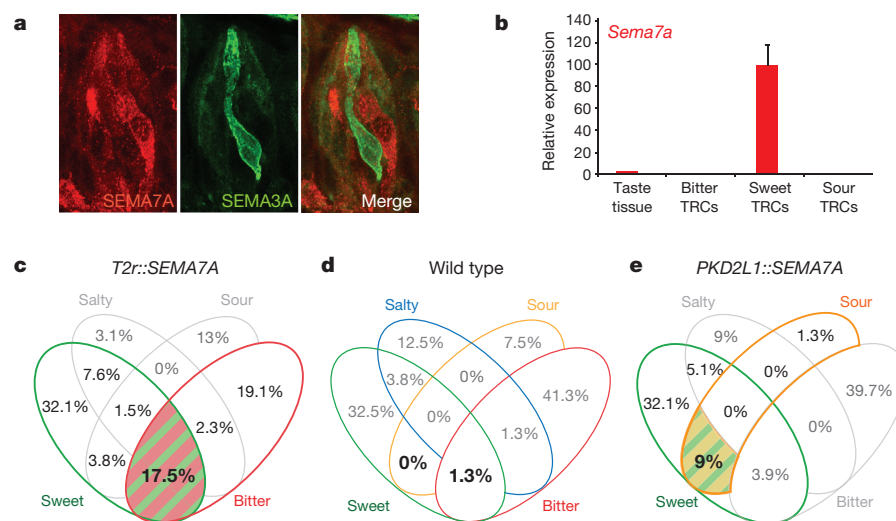


Figure 4 | Rewiring of sweet geniculate ganglion neurons. **a**, Confocal microscopy images of a taste bud showing expression of *SEMA7A* (red) and *SEMA3A* (*Sema3a-cre;Rosa-YFP* reporter line, green). **b**, Quantitative RT–PCR demonstrating highly selective expression of *Sema7a* transcripts in sweet TRCs; data are presented as mean \pm s.e.m.; $n = 3$. **c–e**, Geniculate ganglion responses show that *SEMA7A* directs sweet neuron connectivity.

c, Mice expressing *SEMA7A* in bitter cells (*T2r::SEMA7A*; $n = 7$ mice, 131 cells). Sweet–bitter multi-tuned cells are highlighted in colour ($P < 0.01$, Fisher’s exact test). **d**, Wild-type mice ($n = 4$ mice, 80 cells). **e**, Mice expressing *SEMA7A* in sour cells (*PKD2L1::SEMA7A*; $n = 4$ mice, 78 cells). Sweet–sour doubly tuned cells are highlighted ($P < 0.01$, Fisher’s exact test). See also Extended Data Table 3.

results demonstrated the selective emergence of a very large number of sweet-responding neurons that are also activated by bitter tastants in the *SEMA7A*-expressing mice (Fig. 4c, d). To investigate whether these findings could be extended to additional classes of TRCs, we next examined sour taste, and generated animals misexpressing *SEMA7A* in sour TRCs. We anticipated that, in this instance, the taste system would be rewired such that sour TRCs are now signalling to sweet ganglion neurons. Indeed, these engineered mice have a pronounced loss of singly tuned sour neurons, with the vast majority of their sour responses in neurons that are also activated by sweet stimuli (Fig. 4e).

The taste system affords the unique opportunity to explore how labelled lines between primary sensory cells and neurons are wired and preserved. At the periphery, five basic classes of TRCs signal to a matching set of ganglion neurons. But how ganglion processes identify their proper TRC partners has remained unclear. The chemoaffinity hypothesis has been a tenet of neuronal connectivity for over 100 years^{27,28}. Yet, despite much effort, there are limited examples in vertebrates where guidance molecules expressed by target cells direct cell to cell connectivity, rather than 'regional' level connectivity²⁹. Because taste cells are assembled into tightly packed taste buds (with a random distribution of TRCs that represent each modality)³⁰, they provide an ideal experimental platform to explore how connectivity rules may operate at a cell-to-cell level. Moreover, as TRCs are constantly renewed during the life of the animal, they require continuous re-establishment of connections between existing ganglion processes and newly born TRCs. Here, we combine single-cell functional imaging and mouse genetics to demonstrate that sweet and bitter TRCs use distinct semaphorins in a deterministic fashion to guide wiring of the peripheral taste system (probably together with other connectivity molecules as part of a multi-component wiring specificity code; see also Extended Data Fig. 2). Our results show how targeted misexpression of even a single connectivity signal alters taste cell–neuronal communication in a predictable fashion (for example, sweet signalling to bitter, or sour to sweet). Together, these studies reveal basic rules of TRC–neuron connectivity, substantiate the labelled-line organization of the taste system, and help to explain how a hardwired sensory system maintains fidelity of signalling in the face of random turnover of receptor cells.

Online Content Methods, along with any additional Extended Data display items and Source Data, are available in the online version of the paper; references unique to these sections appear only in the online paper.

Received 14 February; accepted 21 June 2017.

Published online 9 August 2017.

- Lindemann, B. Receptors and transduction in taste. *Nature* **413**, 219–225 (2001).
- Yarmolinsky, D. A., Zuker, C. S. & Ryba, N. J. P. Common sense about taste: from mammals to insects. *Cell* **139**, 234–244 (2009).
- Barlow, L. A. & Klein, O. D. Developing and regenerating a sense of taste. *Curr. Top. Dev. Biol.* **111**, 401–419 (2015).
- Zipursky, S. L. & Sanes, J. R. Chemoaffinity revisited: dscams, protocadherins, and neural circuit assembly. *Cell* **143**, 343–353 (2010).
- Yoshida, Y. Semaphorin signaling in vertebrate neural circuit assembly. *Front. Mol. Neurosci.* **5**, 71 (2012).
- Pasterkamp, R. J. Getting neural circuits into shape with semaphorins. *Nat. Rev. Neurosci.* **13**, 605–618 (2012).
- Wang, F., Nemes, A., Mendelsohn, M. & Axel, R. Odorant receptors govern the formation of a precise topographic map. *Cell* **93**, 47–60 (1998).
- Komiyama, T. & Luo, L. Development of wiring specificity in the olfactory system. *Curr. Opin. Neurobiol.* **16**, 67–73 (2006).

- Zhao, G. Q. *et al.* The receptors for mammalian sweet and umami taste. *Cell* **115**, 255–266 (2003).
- Mueller, K. L. *et al.* The receptors and coding logic for bitter taste. *Nature* **434**, 225–229 (2005).
- Hayashi, S. & Takeichi, M. Emerging roles of protocadherins: from self-avoidance to enhancement of motility. *J. Cell Sci.* **128**, 1455–1464 (2015).
- Zipursky, S. L. & Grueber, W. B. The molecular basis of self-avoidance. *Annu. Rev. Neurosci.* **36**, 547–568 (2013).
- Koropouli, E. & Kolodkin, A. L. Semaphorins and the dynamic regulation of synapse assembly, refinement, and function. *Curr. Opin. Neurobiol.* **27**, 1–7 (2014).
- Coate, T. M., Spita, N. A., Zhang, K. D., Isgrig, K. T. & Kelley, M. W. Neuropilin-2/semaphorin-3F-mediated repulsion promotes inner hair cell innervation by spiral ganglion neurons. *eLife* **4**, e07830 (2015).
- Tran, T. S. *et al.* Secreted semaphorins control spine distribution and morphogenesis in the postnatal CNS. *Nature* **462**, 1065–1069 (2009).
- Luo, Y., Raible, D. & Raper, J. A. Collapsin: a protein in brain that induces the collapse and paralysis of neuronal growth cones. *Cell* **75**, 217–227 (1993).
- Messersmith, E. K. *et al.* Semaphorin III can function as a selective chemorepellent to pattern sensory projections in the spinal cord. *Neuron* **14**, 949–959 (1995).
- Song, H. *et al.* Conversion of neuronal growth cone responses from repulsion to attraction by cyclic nucleotides. *Science* **281**, 1515–1518 (1998).
- Polleux, F., Morrow, T. & Ghosh, A. Semaphorin 3A is a chemoattractant for cortical apical dendrites. *Nature* **404**, 567–573 (2000).
- Telley, L. *et al.* Dual function of NRP1 in axon guidance and subcellular target recognition in cerebellum. *Neuron* **91**, 1276–1291 (2016).
- Barretto, R. P. *et al.* The neural representation of taste quality at the periphery. *Nature* **517**, 373–376 (2015).
- Wu, A., Dvoryanchikov, G., Pereira, E., Chaudhari, N. & Roper, S. D. Breadth of tuning in taste afferent neurons varies with stimulus strength. *Nat. Commun.* **6**, 8171 (2015).
- Taniguchi, M. *et al.* Disruption of semaphorin III/D gene causes severe abnormality in peripheral nerve projection. *Neuron* **19**, 519–530 (1997).
- Merte, J. *et al.* A forward genetic screen in mice identifies *Sema3A*^{K108N}, which binds to neuropilin-1 but cannot signal. *J. Neurosci.* **30**, 5767–5775 (2010).
- Carcea, I. *et al.* Maturation of cortical circuits requires semaphorin 7A. *Proc. Natl Acad. Sci. USA* **111**, 13978–13983 (2014).
- Pasterkamp, R. J., Peschon, J. J., Spriggs, M. K. & Kolodkin, A. L. Semaphorin 7A promotes axon outgrowth through integrins and MAPKs. *Nature* **424**, 398–405 (2003).
- Langley, J. N. Note on regeneration of prae-ganglionic fibres of the sympathetic. *J. Physiol. (Lond.)* **18**, 280–284 (1895).
- Sperry, R. W. Chemoaffinity in the orderly growth of nerve fiber patterns and connections. *Proc. Natl Acad. Sci. USA* **50**, 703–710 (1963).
- Sanes, J. R. & Yamagata, M. Many paths to synaptic specificity. *Annu. Rev. Cell Dev. Biol.* **25**, 161–195 (2009).
- Zaidi, F. N. & Whitehead, M. C. Discrete innervation of murine taste buds by peripheral taste neurons. *J. Neurosci.* **26**, 8243–8253 (2006).

Supplementary Information is available in the online version of the paper.

Acknowledgements We thank T. Yagi for providing the floxed *Sema3a* mice, R. Barretto and D. Yarmolinsky for help with *in vivo* imaging and analysis, and Z. Wu, I. Schieren and S. O’Keeffe for advice and expert technical support. We also thank N. Balaskas and the members of the Zuker laboratory for helpful comments and suggestions. Research reported in this publication was supported by the National Institute On Drug Abuse of the National Institutes of Health under Award Number R01DA035025 (C.S.Z.) and in part by the Intramural Research Program of the NIH, NIDCR (N.J.P.R.). L.J.M. was an HHMI Fellow of the Jane Coffin Childs Memorial Fund. C.S.Z. is an investigator of the Howard Hughes Medical Institute and a Senior Fellow at Janelia Farm Research Campus.

Author Contributions H.L. and L.J.M. designed the study, carried out the experiments, analysed data and wrote the paper, C.A.P. performed experiments, C.S.Z. and N.J.P.R. designed the study, analysed data and wrote the paper.

Author Information Reprints and permissions information is available at www.nature.com/reprints. The authors declare no competing financial interests. Readers are welcome to comment on the online version of the paper. Publisher’s note: Springer Nature remains neutral with regard to jurisdictional claims in published maps and institutional affiliations. Correspondence and requests for materials should be addressed to C.S.Z. (cz2195@columbia.edu).

METHODS

Animals. All procedures were carried out in accordance with the US National Institutes of Health (NIH) guidelines for the care and use of laboratory animals, and were approved by the Institutional Animal Care and Use Committee at Columbia University. Adult animals ranging from 2 to 12 months of age and from both genders were used in all experiments. No statistical methods were used to predetermine sample size, and investigators were not blinded to group allocation. No method of randomization was used to determine how animals were allocated to experimental groups. Transgenic mice were engineered by pronuclear injection of recombinant BAC constructs. Flag tags were added to SEMA3A and SEMA7A misexpression constructs using Gibson cloning (NEB) to detect misexpressed proteins. *T1r3::SEMA3A* was generated by insertion of human *SEMA3A* (GE Dharmacon, MHS6278-211690268) into the *T1r3* start codon in BAC RP23-236C12 (see Extended Data Fig. 3 for validation of the new mouse lines). *Sema3a-cre* was generated by recombining a Cre cassette at the start codon of the *Sema3a* gene in BAC RP23-151O24. *T2r::SEMA7A* was generated by recombining human *SEMA7A* cDNA (GE Dharmacon, MHS6278-202857566) to the start codon of *T2r19* gene in BAC RP23-325J2. *Pkd2l1::SEMA7A* was engineered by insertion of the human *SEMA7A* into the *Pkd2l1* start codon in BAC RP23-297K23. *Trpm5-BFP* was generated by insertion of p2A-BFP cassette (Evrogen) to replace the *Trpm5* stop codon in BAC RP23-366M16. *Pkd2l1-tdTomato* was generated by insertion of a tdTomato cassette at the *Pkd2l1* start codon in BAC RP23-297K23. Other mouse strains used were previously described: *T2r-GFP* (*T2r32-Sapphire*)³¹, *Sema3a^{lox/lox}* (RIKEN, RBRC01106)²³, *Sema3a^{M/M}* (JAX Stock 014646)²⁴, *Rosa-YFP* (JAX Stock 6148). All strains were backcrossed (for at least two generations) and maintained on a C57BL/6 background.

TRC isolation and RNA-seq. Tongues were extracted from euthanized mice expressing fluorescent reporters for specific TRCs and injected with a dispase/collagenase (Roche) enzyme cocktail. After a 10-min incubation in 3°C, lingual epithelia were carefully peeled off from the muscle layer. Peeled lingual epithelia were placed in 0.25% Trypsin-EDTA (Invitrogen) for 15 min at 37°C, triturated and sequentially passed through 70- μ m and 40- μ m filters (Corning) to obtain single cells. Fluorescently labelled TRCs were isolated from dissociated cells using a fluorescence activated cell sorter (MoFlo Astrios, Beckman Coulter).

Bitter and sweet/umami TRC populations were isolated from a mouse line that has both *T2r-GFP* and *Trpm5-BFP* transgenes (labelling sweet, umami and bitter TRCs)³². From these mice, GFP⁺BFP⁺ (bitter TRCs) or GFP⁺BFP⁻ TRCs (sweet/umami) were sorted by FACS into tubes containing cell lysis buffer. Each pool contained about 500 cells. Total RNA was extracted using the Arcturus PicoPure RNA Isolation kit (Thermo Fisher) according to the manufacturer's instructions and was immediately used for RNA-seq library generation with the Ovation RNA-Seq System v.2 (NuGEN). RNA-seq and analysis were performed by the Columbia Genome Center core facility. The RNA-seq experiment was performed in three biological replicates.

Quantitative RT-PCR. Samples were from circumvallate papilla (taste tissue), lingual epithelia, T2R-GFP⁺TRPM5-BFP⁺ (bitter) TRCs, T2R-GFP⁻TRPM5-BFP⁺ (sweet/umami) TRCs, and PKD2L1-tdTomato⁺ (sour) TRCs. Total RNA from each sample was isolated and complementary DNA prepared using the Ovation RNA-Seq System v.2 kit. Quantitative reverse-transcription PCR (qRT-PCR) was performed on a StepOne Plus (Applied Biosystems) cycler using the Taqman Gene Expression system (Thermo Fisher). Taqman probes were as follows: *T1r3* (Mm0167446_g1), *T2r5* (Mm0098502_s1), *Pkd2l1* (Mm00619572_m1), *Sema3a* (Mm01230889_m1), *Bdnf* (Mm04230607_s1), *Slit2* (Mm01216521_m1), *Dscaml1* (Mm01174253_m1), *Pcdhgb7* (Mm04209449_m1), *Tspan18* (Mm00806028_m1), *Nrxn3* (Mm04279482_m1), *Sema7a* (Mm00441361_m1) and *Actb* (Mm01205647_g1). For detection of semaphorin receptors, samples were from geniculate ganglia and fungiform papillae. qRT-PCR was performed using VeriQuest SYBR green master mix (Thermo Fisher) with the following primer pairs: *Plxn4* (ACCCGGATCTTCTCAGCTT and CTCTGGGAGTTTCCGAAATG), *Plxn1* (CAGTTTTCAAAGCTCCAGC and TTGCAAAGTGCAGTAAACGG), *Irgb1* (GGCCAAATACAGAAACAATCAA and ACACCGACCCGAGACCT), *Nrp1* (AGGTGCAATCTCCACAGA and CCGGAACCTACCCAGAGAAAT), *Actb* (ATGGAGGGGAATACAGCC and TTCTTTGCAGCTCTCAGTT), *P2x3* (TGATGGTGGGAATGATGTTG and TGTTTCCCTGGCTACAAC), *T1r3* (CTTTTCTCTGGGACCCTG and AAAGGGCTTTCATCTCTGCT). Experiments were performed in three biological replicates. Data were normalized to β -actin.

Immunostaining. Animals were euthanized and fixed by intracardiac perfusion with a 4% paraformaldehyde solution. Tongues were excised and placed in 30% sucrose solution overnight at 4°C for cryoprotection. Tissues were embedded in OCT compound and sectioned at 30- μ m thickness on a cryostat. Sections were washed in PBS with 0.1% Triton X-100 (PBST), blocked with 10% donkey serum in PBST, incubated with primary antibodies overnight at 4°C, and incubated with

fluorescence-tagged secondary antibodies (Jackson ImmunoResearch) for 2 h at room temperature. Primary antibodies used were: anti-SEMA7A (R&D Systems AF1835; 1:300 dilution), anti-Flag (Sigma F7425; 1:1,000 dilution), anti-T1R3 (Santa Cruz Biotechnology sc-22458; 1:500 dilution), anti-CAR4 (R&D Systems AF2414; 1:500 dilution), anti-PLC β 2 (Santa Cruz Biotechnology sc-206; 1:1,000 dilution), anti-GFP (Abcam ab13970; 1:500 dilution), anti-Nrp1 (R&D Systems AF566; 1:200 dilution), and anti-PlxnC1 (R&D Systems AF5375; 1:200 dilution). **Viral delivery of GCaMP sensors.** Mice were anaesthetized with ketamine and xylazine (100 mg kg⁻¹ and 10 mg kg⁻¹, intraperitoneal), with subsequent booster doses to maintain depth of anaesthesia. Body temperature was controlled using a closed-loop heating system. A small craniotomy (<1 mm diameter) centred approximately 6.5 mm dorsal to bregma and 1.25 mm from the midline was performed. AAV virus carrying AAV2.1-hSyn-GCaMP6s (Penn Vector Core) was delivered to the brain at three locations along the rostrocaudal axis: 1.25 mm/–4.0 mm (lateral coordinate relative to bregma/inferior coordinate relative to the dura), and –6.3 mm/–6.5 mm/–6.7 mm (anterior coordinates relative to bregma); approximately 200 nl was delivered per injection. After incision closure and recovery from surgery, mice were housed in their home cages for at least one week before imaging.

Calcium imaging. A metal bar was affixed to the dorsal cranium of an anaesthetized mouse (see above) with Vetbond Tissue Adhesive (3M) and dental cement as described previously²¹. The mouse was positioned in a supine position, and its head rigidly secured using a metal bar. A tracheotomy was performed to maintain a clear airway during tastant delivery to the oral cavity. The surgical strategy used to image the geniculate ganglion *in vivo* was as previously described²¹. Imaging data was obtained using an Evolve 512 EMCCD camera (Photometrics). All images were acquired at 5 Hz, with 10 \times magnification. A single field of view was analysed for each ganglion.

Tastants were delivered (5–10 ml per min) using silicon tubing positioned approximately 8 mm inside the oral cavity, dorsal to the tongue. Tastants dissolved in water were delivered for 2 s each in serial order, interspersed with 13 s of water rinse. Images were acquired during epochs of continuous irrigation. The concentrations (and application order) of tastants used were: aceulfame K (AceK), 30 mM; quinine hydrochloride, 5 mM; NaCl, 60 mM; monopotassium glutamate + inosine monophosphate, 50 mM + 1 mM, respectively; citric acid, 50 mM. Additional tastants: sucrose (300 mM) and cycloheximide (100 μ M).

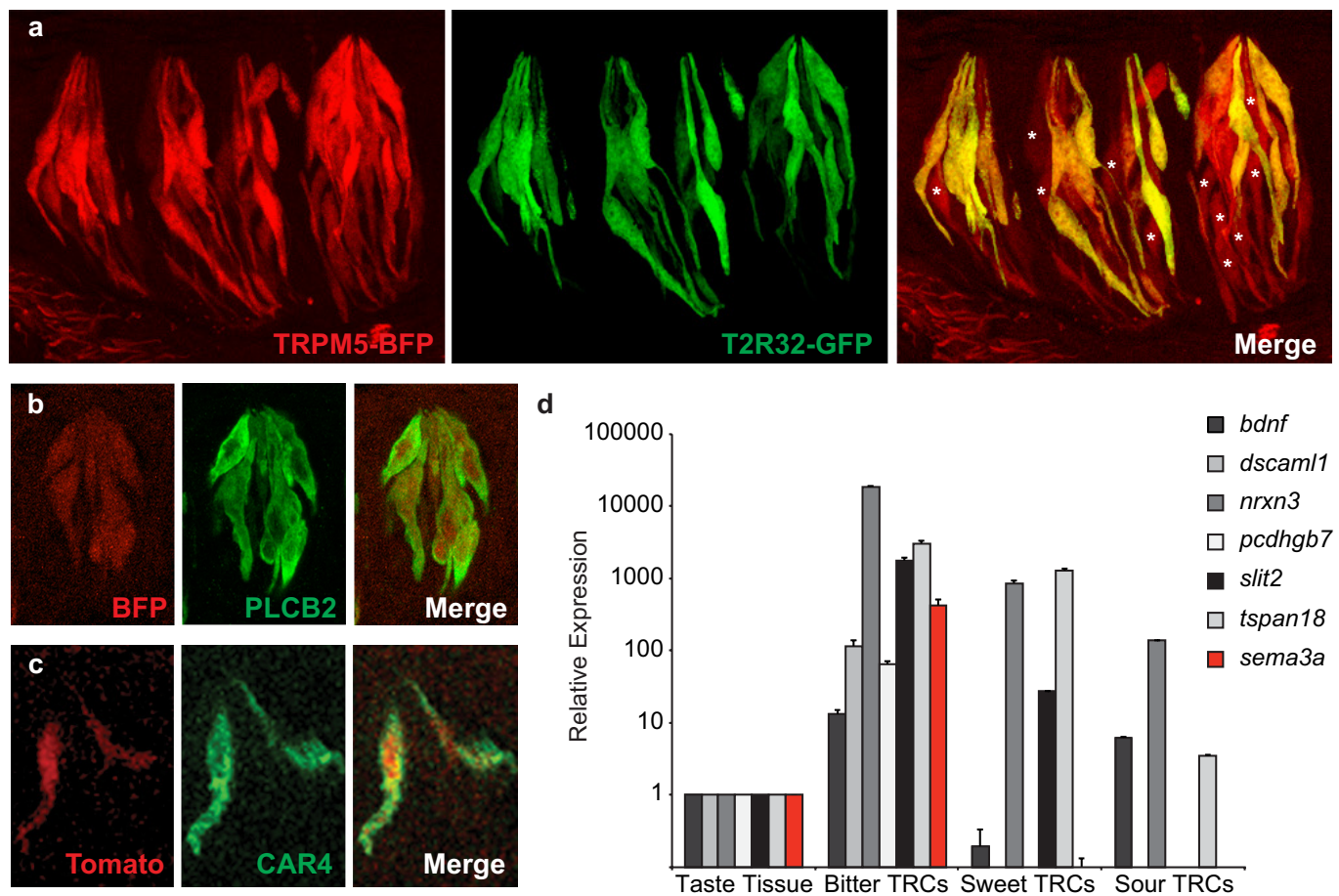
Calcium imaging data analysis. Imaging data were analysed using custom software implemented in MATLAB (MathWorks) as described previously³³. For each field of view, all image stacks were first registered for motion correction using Image Stabilizer for ImageJ²¹. To identify neurons, maps of peak activity (maximal pixel intensity over mean pixel intensity) median filtered, thresholded and separated by watershed segmentation to create candidate regions of interest representing active neurons, which were reviewed manually to identify ROIs for all active neurons. Fluorescence traces for each region of interest were normalized to neighbourhood fluorescence intensity (defined as the average intensity within a two-cell radius distance of each cell, excluding all other defined ROIs) to correct for neuropil signal³³. Calcium transients were automatically detected as fluorescence excursions of >3-fold above noise (defined as median average deviation). We visually scored cells, by directly observing the aligned image data displayed as a relative fluorescence movie, as well as the putative cells' fluorescence time series²¹. Note that if a ganglion neuron were completely miswired such that it lost its original tuning identity, it would not show up as multi-tuned, thus under-representing the extent of rewiring. To ensure that signals originated from a single neuron, and not from closely adjacent cells or out-of-focus fluorescence from deeper cell layers, we examined the correlation of pixels in the neighbourhood of each ROI for each calcium transient, discarding from analysis any neuron contaminated by outside signals. Fisher's exact test was used to determine statistical significance between cell populations.

Behavioural assays. Taste behaviour was assayed using a short-term assay that directly measures taste preferences by counting immediate licking responses in a multi-channel gustometer (Davis MS160-Mouse gustometer; DiLog Instruments)³². Mice were water restricted for 24 h before gustometer training. For 2–3 days, mice were acclimated to the gustometer, and trained to lick water from the gustometer spouts. After 10 min in the gustometer 2 \times per day, the mice were given 1 h access to water in their home cage. On testing days, the mice were placed individually into the gustometer chamber, and presented with water or two different concentrations of a given bitter tastant at random (quinine hydrochloride, denatonium, or 6-n-propylthiouracil (PROP)). During each presentation, the shutter opens, and the mouse has a 60 s window to lick the spout to continue the trial, otherwise it proceeded to the next trial. After the first lick is detected, the mouse is given 10 s to lick before the shutter closes, and the next presentation starts. The number of licks, inter-lick interval, and lick latency are recorded for each presentation. The duration of the experiment was 20 min.

Nerve recordings. Lingual stimulation and recording procedures were carried out as described previously³²; data analysis used the integrated response during the 5 s of tastant stimulation. Compounds used for nerve recordings were: acesulfame K (30 mM); quinine (0.625–5 mM), and NaCl (60 mM). Data were analysed for statistical significance using an unpaired, one-tailed Student's *t*-test and 95% confidence limits.

Data availability. The data that support the findings of this study are available from the corresponding author upon reasonable request. RNA-seq data that support the findings of this study have been deposited in the NCBI Sequence Read Archive (SRA) with the accession code PRJNA390545.

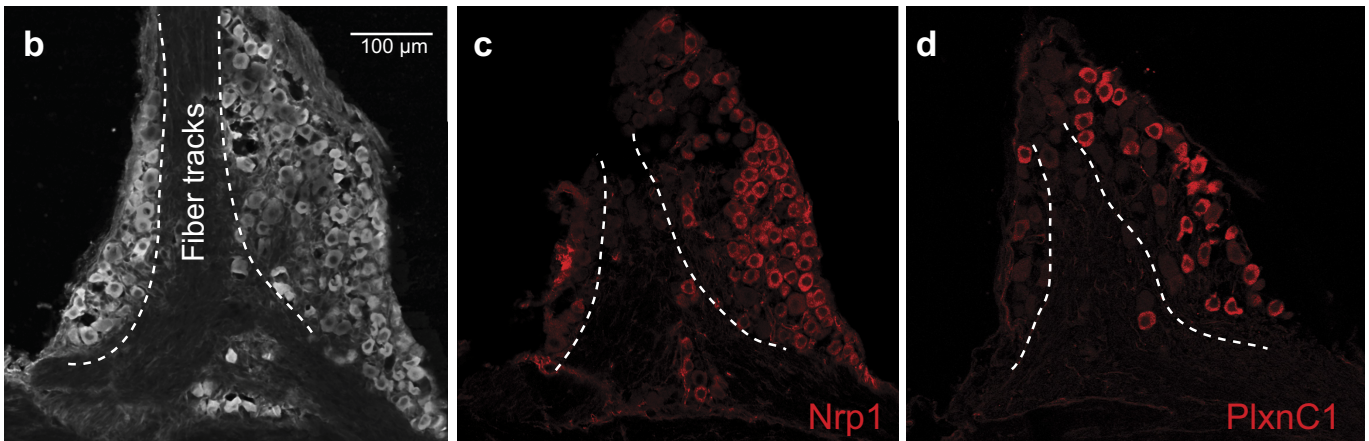
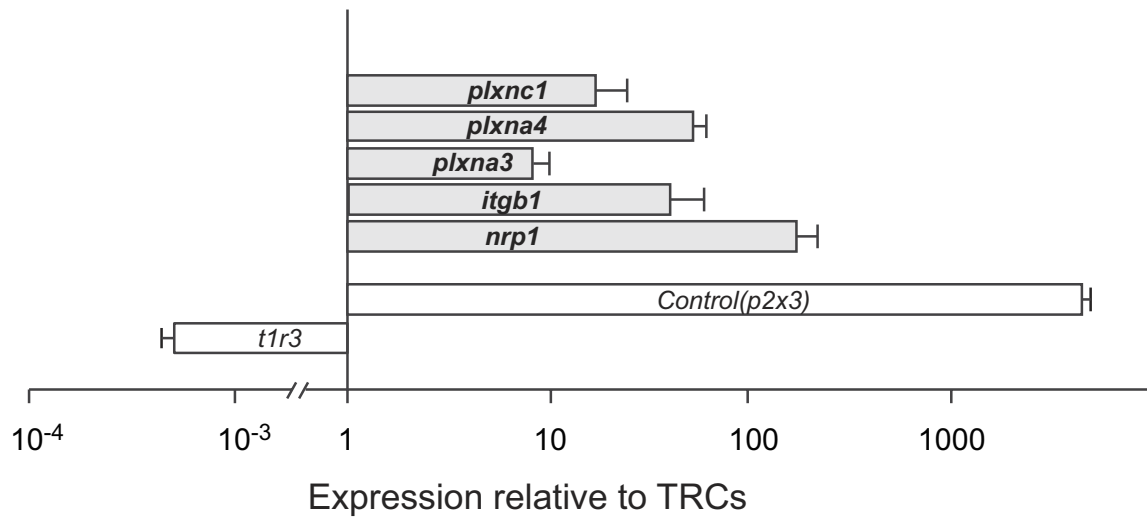
31. Oka, Y., Butnaru, M., von Buchholtz, L., Ryba, N. J. P. & Zuker, C. S. High salt recruits aversive taste pathways. *Nature* **494**, 472–475 (2013).
32. Zhang, Y. *et al.* Coding of sweet, bitter, and umami tastes: different receptor cells sharing similar signaling pathways. *Cell* **112**, 293–301 (2003).
33. Yarmolinsky, D. A. *et al.* Coding and plasticity in the mammalian thermosensory system. *Neuron* **92**, 1079–1092 (2016).
34. Chandrashekar, J. *et al.* The taste of carbonation. *Science* **326**, 443–445 (2009).
35. Vandenbeuch, A. *et al.* Postsynaptic P2X3-containing receptors in gustatory nerve fibres mediate responses to all taste qualities in mice. *J. Physiol. (Lond.)* **593**, 1113–1125 (2015).



Extended Data Figure 1 | Expression profiling of fluorescently labelled TRC populations identifies candidate signalling molecules enriched in bitter TRCs. **a**, Confocal microscopy images of circumvallate papilla taste buds from a TRPM5-BFP (labelling sweet and bitter TRCs³², pseudo-coloured red); T2R32-GFP (labelling bitter TRCs) double-labelled transgenic mouse. These are the animals used in the profiling of sweet/umami and bitter TRCs. Note the expected co-expression of bitter taste receptors and a subset of TRPM5⁺ cells (right; TRPM5⁺, but T2R⁻ TRCs are indicated by asterisks). **b**, Taste bud from a TRPM5-BFP transgenic

mouse showing co-expression of the BFP reporter (pseudo-coloured red) and PLCβ2 (a marker of sweet, umami and bitter TRCs³², green). **c**, Taste bud from a PKD2L1-TdTomato transgenic animal demonstrating expression of the TdTomato reporter (red) in sour TRCs (marked by CAR4 (ref. 34), green). **d**, qRT-PCR illustrating the relative expression of several candidate connectivity molecules in bitter, sweet and sour TRCs. Data are presented as mean + s.e.m. relative to the expression levels in the whole circumvallate papilla (referred to as taste tissue); $n = 3$.

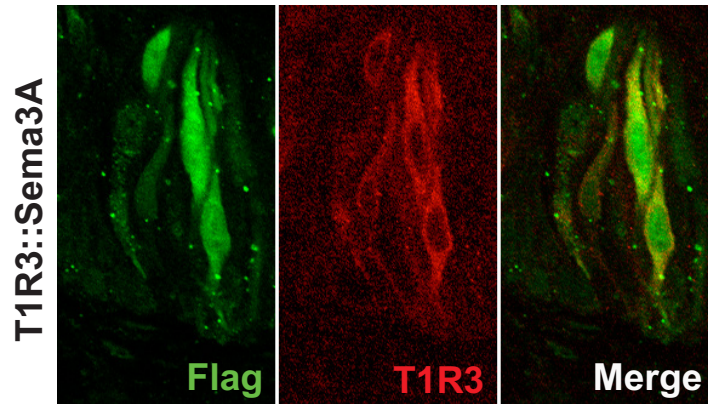
a



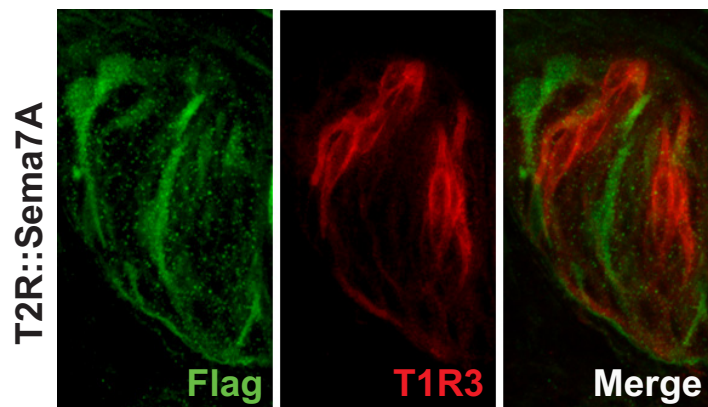
Extended Data Figure 2 | Expression of semaphorin receptors in geniculate ganglion neurons. **a**, qRT-PCR analysis showing expression of candidate SEMA3A receptors^{5,6} (*Nrp1*, *Plxna3* and *Plxna4*) and SEMA7A receptors^{5,6} (*Itgb1* and *Plxnc1*) in the geniculate ganglia. *P2rx3* (also known as *P2rx3*) and *T1r3* were used as controls for geniculate ganglia³⁵ and TRC⁹ tissue integrity, respectively. *Nrp1*, neuropilin 1; *Plxna3*, plexin A3;

Plxna4, plexin A4; *Itgb1*, integrin $\beta 1$; *Plxnc1*, plexin C1. Data are presented for each gene as its relative abundance in the ganglia compared to TRCs. Values are mean + s.e.m. ($n = 3$). **b–d**, Confocal microscopy images of immunostaining illustrating the expression of NRP1 (**c**) and PLXNC1 (**d**) in subsets of geniculate ganglion neurons. **b**, The anatomy of the ganglion highlighting the location of fibre tracks.

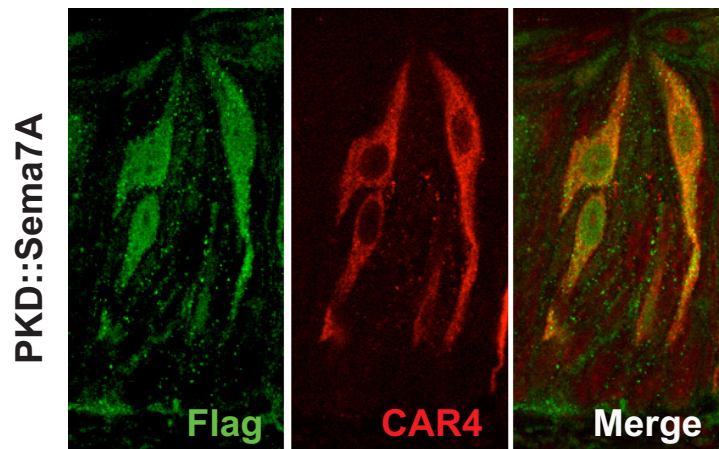
a



b

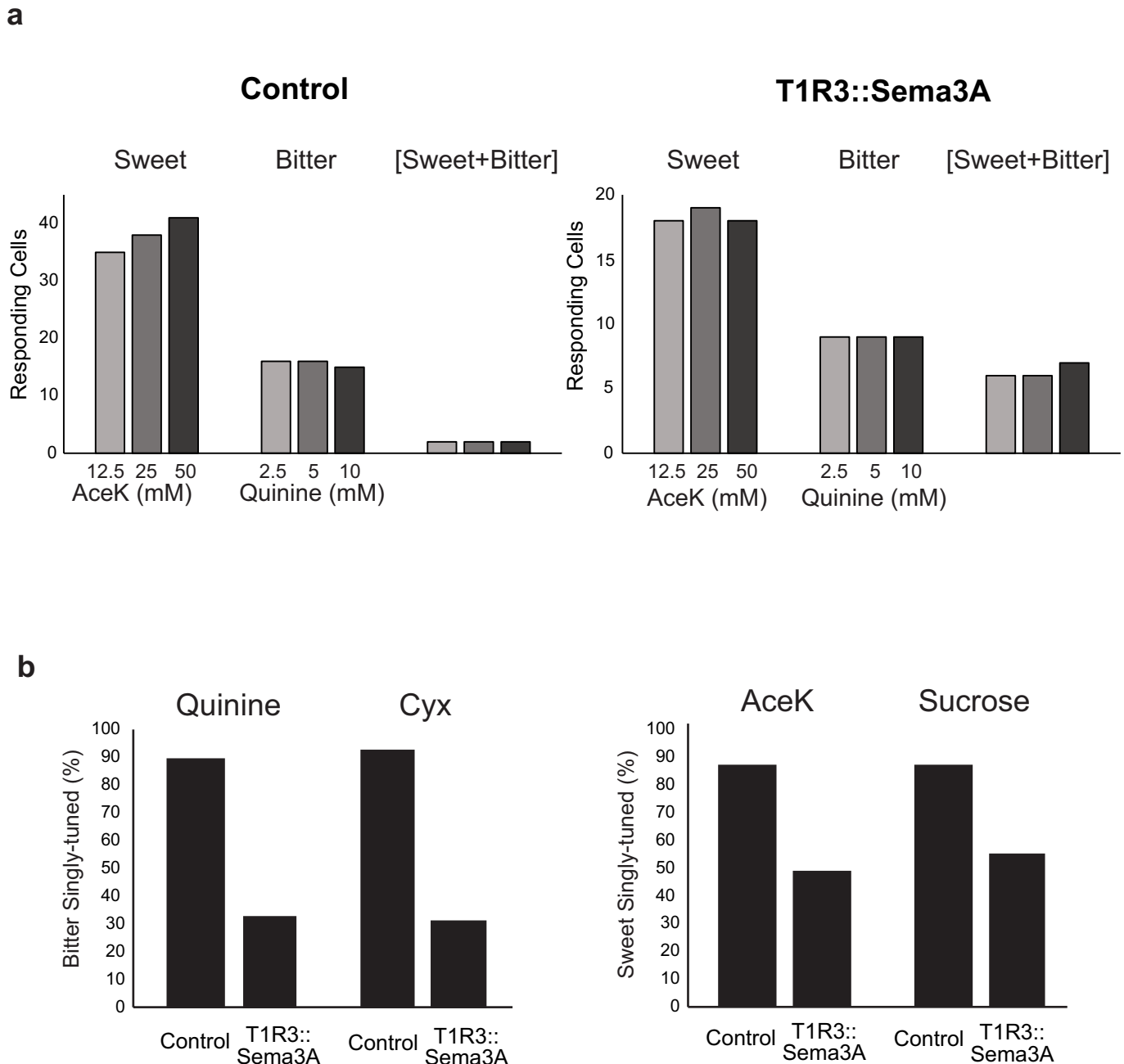


c



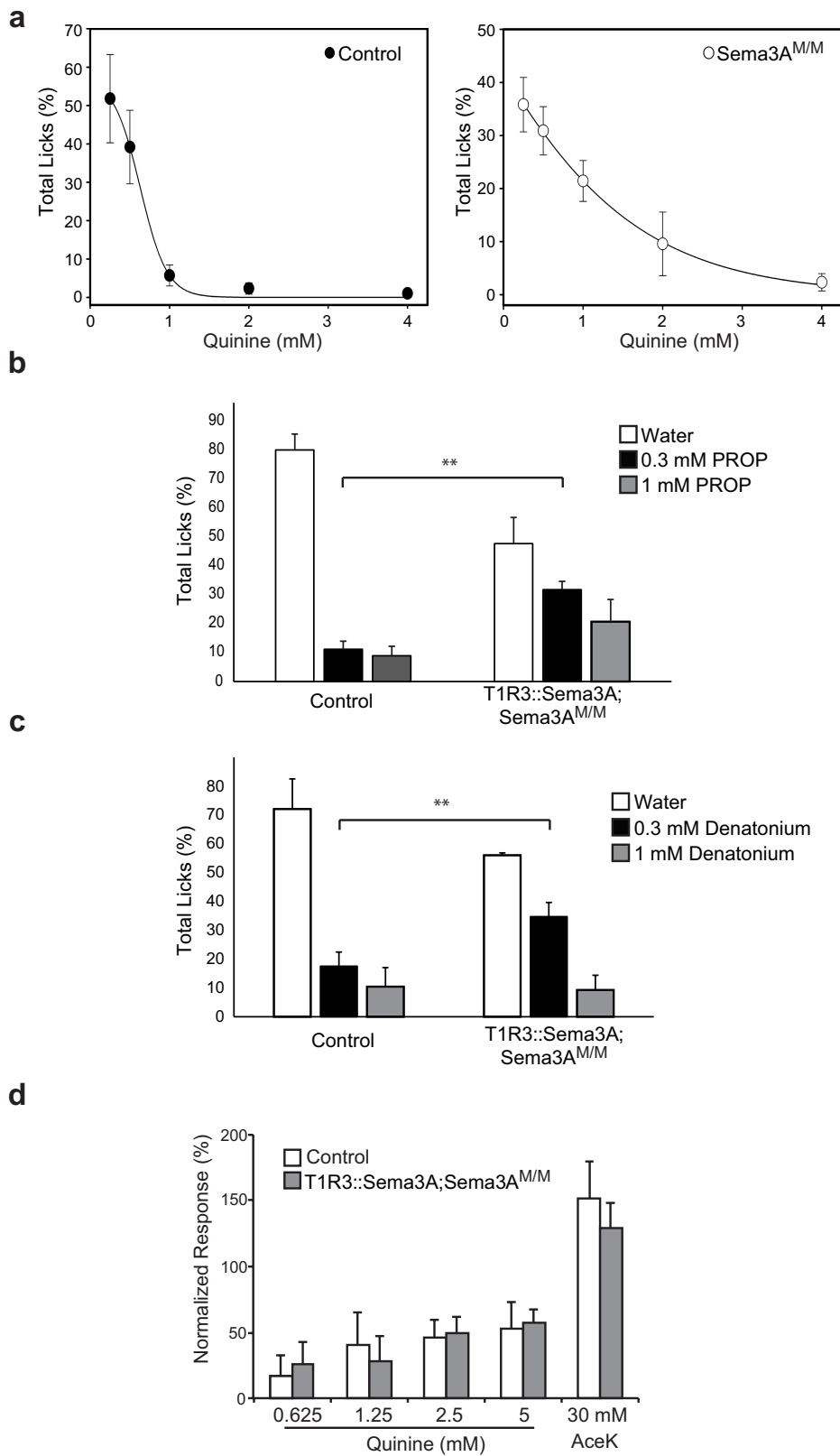
Extended Data Figure 3 | Targeted misexpression of SEMA3A and SEMA7A. a, Confocal microscopy images of circumvallate papilla taste buds from a *T1r3::SEMA3A* mouse demonstrating transgene expression (marked by Flag tag; green) in T1R3-expressing TRCs (red). b, The

SEMA7A transgene of *T2r::SEMA7A* animals (green) is expressed in a subset of TRCs not overlapping with T1R3 (red). c, *SEMA7A* (green) in *Pkd21l1::SEMA7A* animals is expressed in sour TRCs (marked by CAR4, red).



Extended Data Figure 4 | Responses of ganglion neurons in *T1r3::SEMA3A* mice. **a**, Dose responses to sweet and bitter in control and *T1r3::SEMA3A* mice. The number of cells that respond at each stimulus concentration is shown, cells are classified by their response profile (that is, sweet-responding, bitter-responding or sweet-bitter responding). Note that the tuning profiles are maintained at all three sweet and bitter concentrations, including extremely high concentrations of bitter¹⁰ and sweet⁹. Control, $n = 58$ cells; *T1r3::SEMA3A*, $n = 34$ cells. **b**, Responses

are similar for different tastants within a modality. Tuning properties of bitter- and sweet-responding neurons in the *T1r3::SEMA3A* animals to two structurally different bitter- and sweet-tasting chemicals are shown. Quinine (5 mM), cycloheximide (Cyx, 100 μ M), AceK (30 mM) and sucrose (300 mM). Control, $n = 178$ bitter-responding cells, $n = 227$ sweet-responding cells (seven mice). *T1r3::SEMA3A*, $n = 130$ bitter-responding cells, $n = 165$ sweet-responding cells (five mice).



Extended Data Figure 5 | See next page for caption.

Extended Data Figure 5 | Aversion to bitter tastants is impaired in *T1r3::SEMA3A;Sema3a^{M/M}* mice. **a**, Dose-response to the bitter quinine in control and *Sema3a^{M/M}*-mutant mice. Animals were tested using a brief-access lick assay as previously described¹⁰. The relative fraction of licks to each concentration of quinine is shown (0.25 mM, 0.5 mM, 1 mM, 2 mM, 4 mM). Control, $n = 4$; *Sema3a^{M/M}*, $n = 5$; mean \pm s.d. **b, c**, Targeting bitter neurons to sweet TRCs results in a significant loss of bitter taste sensitivity (see also Fig. 3f). **b**, The graphs show the relative fraction of licks to water and to two different concentrations of PROP in control and *T1r3::SEMA3A;Sema3a^{M/M}* animals. **c**, The graphs show the relative fraction of licks to water and to two different concentrations of denatonium in control and

T1r3::SEMA3A;Sema3a^{M/M} animals. $n = 3$, mean \pm s.d., $**P < 0.01$, Student's two-tailed, unpaired t -test. **d**, Chorda tympani whole-nerve recording³² in control and *T1r3::SEMA3A;Sema3a^{M/M}*-mutant mice. Responses were normalized to 60 mM NaCl ($n = 3$, mean \pm s.d.). Note that whole-nerve responses to bitter and sweet are unchanged, probably because nerve recording measures bulk neural activity, further highlighting the importance of recording single-neuron activity; GCaMP-based imaging of ganglion activity is markedly more informative than whole-nerve, or even single-fibre physiological recordings, because it allows simultaneous sampling of large numbers of neurons with single-cell selectivity.

Extended Data Table 1 | The distribution of geniculate ganglion neurons according to their responses to each of the five basic taste qualities in *SEMA3A*-mutant and control animals

Response Profile	Control (13 mice)	Sema3AKO (5 mice)
Sweet	84	63
Bitter	94	48
Sour	25	11
Umami	2	0
Salty	24	4
Bitter-Sweet	2	15
Bitter-Umami	1	3
Bitter-Salty	2	9
Bitter-Sweet-Salty	2	5
Bitter-Sweet-Umami	0	2
Bitter-Salty-Umami	0	5
Bitter-Sweet-Salty-Umami	0	6
Sweet-Sour	3	4
Sweet-Umami	5	3
Sweet-Salty	7	3
Sweet-Salty-Sour	1	1
Salty-Sour	2	4
Total cells	254	186

All responsive neurons are included in the table. The numbers of cells responding to the various stimuli in *SEMA3A*-mutant animals and their littermate controls are shown; all data are included in Fig. 2. Note that because bitter-sour-tuned neurons reflect the activation of T2Rs (see ref. 21), they were grouped in the table and in Fig. 2.

Extended Data Table 2 | The distribution of geniculate ganglion neurons according to their responses to each of the five basic taste qualities in *T1r3::SEMA3A*-transgenic and control animals

Response profile	Control (9 mice)	T1R3::Sema3A (6 mice)
Sweet	94	80
Bitter	89	69
Sour	15	19
Umami	2	2
Salty	21	17
Bitter-Sweet	4	43
Bitter-Umami	0	0
Bitter-Salty	2	4
Bitter-Sweet-Salty	1	10
Bitter-Sweet-Umami	2	3
Bitter-Salty-Umami	0	0
Bitter-Sweet-Salty-Umami	0	1
Sweet-Sour	2	8
Sweet-Umami	7	4
Sweet-Salty	3	12
Sweet-Salty-Sour	0	2
Sweet-Salty-Umami	0	1
Sweet-Salty-Umami-Sour	0	1
Salty-Sour	4	3
Salty-Umami	1	0
Salty-Umami-Sour	0	0
Total cells	247	279

The numbers of cells responding to the various stimuli are shown. All data are included in Fig. 3. Note that because bitter-sour neurons reflect responses of T2Rs (see ref. 21), they were grouped.

Extended Data Table 3 | The distribution of geniculate ganglion neurons according to their responses to each of the five basic taste qualities in *T2r::SEMA7A*, wild-type controls and *Pkd2l1::SEMA7A*-transgenic animals

Response profile	T2R::Sema7A (7 mice)	Wildtype (4 mice)	PKD2L1::Sema7A (4 mice)
Sweet	27.5	31.3	30.8
Bitter	19.1	41.3	39.7
Sour	13.0	7.5	1.3
Umami	0	1.3	0
Salty	3.1	12.5	9
Sweet-Bitter	13.0	0	2.6
Sweet-Sour	3.8	0	9
Bitter-Umami	0	1.3	0
Bitter-Salty	2.3	1.3	0
Bitter-Sweet-Salty	2.3	0	0
Bitter-Sweet-Umami	0.8	0	0
Bitter-Salty-Umami	0.8	0	0
Bitter-Sweet-Salty-Umami	0.8	0	1.3
Sweet-Umami	4.6	0	1.3
Sweet-Salty	7.6	3.8	5.1
Sweet-Salty-Sour	1.5	0	0
Total cells	131	80	78

Because of differences in total numbers of cells between the genotypes, the data are presented as percentage (%) of cells responding to the various stimuli. All data are included in Fig. 4. Note that bitter-sour neurons reflect the activation of T2Rs (see ref. 21), and were grouped in Fig. 4.

Life Sciences Reporting Summary

Nature Research wishes to improve the reproducibility of the work that we publish. This form is intended for publication with all accepted life science papers and provides structure for consistency and transparency in reporting. Every life science submission will use this form; some list items might not apply to an individual manuscript, but all fields must be completed for clarity.

For further information on the points included in this form, see [Reporting Life Sciences Research](#). For further information on Nature Research policies, including our [data availability policy](#), see [Authors & Referees](#) and the [Editorial Policy Checklist](#).

▶ Experimental design

1. Sample size

Describe how sample size was determined.

No methods were used to pre-determine sample size. For geniculate imaging data, at least 4 mice were imaged per group.

2. Data exclusions

Describe any data exclusions.

No data were excluded.

3. Replication

Describe whether the experimental findings were reliably reproduced.

All attempts at replication were successful.

4. Randomization

Describe how samples/organisms/participants were allocated into experimental groups.

No randomization was used.

5. Blinding

Describe whether the investigators were blinded to group allocation during data collection and/or analysis.

No blinding was used.

Note: all studies involving animals and/or human research participants must disclose whether blinding and randomization were used.

6. Statistical parameters

For all figures and tables that use statistical methods, confirm that the following items are present in relevant figure legends (or in the Methods section if additional space is needed).

n/a Confirmed

- The exact sample size (n) for each experimental group/condition, given as a discrete number and unit of measurement (animals, litters, cultures, etc.)
- A description of how samples were collected, noting whether measurements were taken from distinct samples or whether the same sample was measured repeatedly
- A statement indicating how many times each experiment was replicated
- The statistical test(s) used and whether they are one- or two-sided (note: only common tests should be described solely by name; more complex techniques should be described in the Methods section)
- A description of any assumptions or corrections, such as an adjustment for multiple comparisons
- The test results (e.g. P values) given as exact values whenever possible and with confidence intervals noted
- A clear description of statistics including central tendency (e.g. median, mean) and variation (e.g. standard deviation, interquartile range)
- Clearly defined error bars

See the web collection on [statistics for biologists](#) for further resources and guidance.

► Software

Policy information about [availability of computer code](#)

7. Software

Describe the software used to analyze the data in this study.

Custom Matlab software and ImageJ was used for motion correction and segmentation to create candidate ROIs (later curated by hand). This software has been previously published: Yarmolinsky et al., Neuron 92, 1079-1092 (2016)

For manuscripts utilizing custom algorithms or software that are central to the paper but not yet described in the published literature, software must be made available to editors and reviewers upon request. We strongly encourage code deposition in a community repository (e.g. GitHub). *Nature Methods* [guidance for providing algorithms and software for publication](#) provides further information on this topic.

► Materials and reagents

Policy information about [availability of materials](#)

8. Materials availability

Indicate whether there are restrictions on availability of unique materials or if these materials are only available for distribution by a for-profit company.

Unique materials (ie transgenic mouse lines) constructed for this study will be made available by the authors. Other materials are commercially available.

9. Antibodies

Describe the antibodies used and how they were validated for use in the system under study (i.e. assay and species).

anti-Sema7a (R&D Systems AF1835)
 anti-FLAG (Sigma F7425)
 anti-T1R3 (Santa Cruz sc-22458)
 anti-Car4 (R&D Systems AF2414)
 anti-Plcb2 (Santa Cruz sc-206)
 anti-GFP (Abcam ab13970)
 anti-Nrp1 (R&D Systems AF566)
 anti-PlxnC1 (R&D Systems AF5375)
 Assayed by immunofluorescence on mouse tissue

10. Eukaryotic cell lines

a. State the source of each eukaryotic cell line used.

No eukaryotic cell lines were used

b. Describe the method of cell line authentication used.

N/A

c. Report whether the cell lines were tested for mycoplasma contamination.

N/A

d. If any of the cell lines used are listed in the database of commonly misidentified cell lines maintained by [ICLAC](#), provide a scientific rationale for their use.

N/A

► Animals and human research participants

Policy information about [studies involving animals](#); when reporting animal research, follow the [ARRIVE guidelines](#)

11. Description of research animals

Provide details on animals and/or animal-derived materials used in the study.

Mus musculus - both males and females 2-12 months old, back-crossed to C57/Bl6

Policy information about [studies involving human research participants](#)

12. Description of human research participants

Describe the covariate-relevant population characteristics of the human research participants.

No human research participants